Electronic Supplementary Information

Tailoring Photocatalytic Activity in Porphyrin-MOFs: The Role of Amine-Functional Pillars in CO_2 Adsorption and Band Structure Modulation

Xing-Zhe Guo‡[a], Chi Cao‡[b], Wei Liu‡[a], Weiwei Xu[a], Nan Ma[a], Xiao-Xia Zhang[c], Jinfa Chang [a], Zihao Xing[a]*

[a] *Key Laboratory of Polyoxometalate and Reticular Material Chemistry of Ministry of Education, Faculty of Chemistry, Northeast Normal University, Changchun 130024, PR China.*
E-mail: xingzh612@nenu.edu.cn
[b] *National Synchrotron Radiation Laboratory, University of Science and Technology of China, Hefei 230029, PR China.*
[c] *School of Chemistry and Chemical Engineering, Fuyang Normal University, Fuyang 030008, PR China.*

1. Materials

Synthesis:

TCPP-Pyz-Co: Tetrakis(4-carboxyphenyl) porphyrin (TCPP, 30 mg, CAS: 14609-54-2, Bidepharm), Pyrazine (Pyz, 20 mg, CAS: 290-37-9, Bidepharm), and $CoCl_2 \cdot 6H_2O$ (20 mg, CAS: 7791-13-1, Aladdin) were added to a 10 mL glass vial. N,N-Dimethylformamide (DMF, 4 mL, CAS: 68-12-2, Aladdin) acetic acid (CH_3COOH, 0.5 mL, CAS: 64-19-7, Aladdin) were subsequently added. The vial was sealed and sonicated until complete dissolution of the solid components was achieved. The resulting solution was then heated at 100 °C for 48 hours in an oven. Following the heating period, the vial was cooled to room temperature, yielding blocky purple-black crystals. The crystals obtained were washed twice with DMF to remove residual reactants and solvent.

TCPP-NH$_2$Pyz-Co: Tetrakis(4-carboxyphenyl)porphyrin (TCPP, 30 mg, CAS: 14609-54-2, Bidepharm), Pyrazinamine (NH_2Pyz, 20 mg, CAS: 5049-61-6, Bidepharm), and $CoCl_2 \cdot 6H_2O$ (20 mg, CAS: 7791-13-1, Aladdin) were added to a 10 mL glass vial. N,N-Dimethylformamide (DMF, 4 mL, CAS: 68-12-2, Aladdin) acetic acid (CH_3COOH, 0.5 mL, CAS: 64-19-7, Aladdin) were subsequently added. The vial was sealed and sonicated until complete dissolution of the solid components was achieved. The resulting solution was then heated at 100 °C for 48 hours in an oven. Following the heating period, the vial was cooled to room temperature, yielding blocky purple-black crystals. The crystals obtained were washed twice with DMF to remove residual reactants and solvent.

Characterizations:

Powder X-ray diffraction (PXRD) data of all samples were recorded on a Rigaku D-Max 2550 diffractometer equipped with Cu-$K\alpha$ radiation (λ = 1.5418 Å). UV-vis spectra were measured on a PE Lambda 750 UV-visible spectrophotometer. FTIR spectra were performed on Thermo Scientific Nicole iS50. Mass spectrometry was performed on an Agilent 8890/5977 GC/MSD gas chromatography-mass spectrometer. Photoluminescence measurements were performed on a Horiba FLUOROMAX-4. N_2 adsorption measurements were carried out using a Quantarome Autosorb-iQ. CO_2 adsorption isotherms were collected on a Quantarome Autosorb-iQ. Energy dispersive spectrometry (EDS) was performed by a X-Max 80T from Oxford. The chemical states of the MOFs were analyzed by X-ray photoelectron spectrometer (XPS, Thermo Fisher Scientific, ESCALAB 250) with an excitation source of Al K_α X-ray (1486.6 eV).

The crystallographic data of TCPP-Pyz-Co and TCPP-NH$_2$Pyz-Co were obtained using a Bruker Apex II CCD diffractometer equipped with graphite-monochromated Mo-$K\alpha$ radiation (λ = 0.71073 Å) at 293 K. The SHELXL-2014 program was adopted to analyse the structure via a direct method and refine it by full matrix least-squares refinements based on F^2 with anisotropic displacement. All non-hydrogen atoms were refined anisotropically. Hydrogen atoms were geometrically placed and refined with isotropic thermal factors. The eventual formula of TCPP-Pyz-Co and TCPP-NH$_2$Pyz-Co were derived from crystallographic data, and elemental and thermogravimetric analysis data. The SQUEEZE program of PLATON was used to remove guests from the disordered species.

Calculation of sorption heat:

The isosteric heats of CO_2 adsorption for TCPP-Pyz-Co and TCPP-NH_2Pyz-Co were calculated by using the Clausius-Clapeyron equation.

$$\ln(P)=Q_{st} \times 1/RT_i +C$$

$$Q_{st}= RT_1T_2/(T_2-T_1) \times (lnP_2-lnP_1)$$

where P is the pressure of the isotherm (kPa), Ti is the temperature of isotherm i (K), R is the gas constant and C is a constant. The Q_{st} is subsequently obtained from the slope of plots of ln (P_i) as a function of 1/T.

Electrochemical Measurements:

The Mott-Schottky spectra, EIS plots, and photocurrent spectra of the samples were measured in Na_2SO_4 solution (0.1 M). The indium tin oxide (ITO) glass (1 × 1 cm^2) was used as the supporting substrate to prepare working electrode. ITO was first washed by ethanol and water under ultrasonic treatment and then dried. Then sample and Nafion ethanol suspension were dropped on the substrate drying it naturally. All electrochemical tests were measured using an electrochemical workstation (CHI660E) on a standard three-electrode cell with photocatalyst-coated ITO as the working electrode, Pt wire as the counter electrode, and Ag/AgCl as the reference electrode.

Photocatalytic Experiments:

The photocatalytic reaction was carried out in a mixed solution of MeCN, H_2O and TEOA (22 mL, MeCN/H_2O/TEOA = 18 : 2 : 2) containing MOFs (5 mg) and $[Ru(bpy)_3]Cl_2$ (20 mg) as the photocatalyst and photosensitizer for CO_2 reduction. The reaction was carried out in a 100 mL sealed custom-made top-illuminated reactor. Before reaction, the reactor was sealed and saturated with ultrapure CO_2 to remove the atmosphere. The reaction was carried out under 300 W Xe lamp with a 420 nm cut-off filter. A cooling circulating water system was used to stabilize the reaction temperature at 25 °C. Photocatalytic reduction products were recorded every one hours for 4 h using Aulight GC equipped with FID and TCD detectors. The recycle test was examined in a completely identical environment. For isotope labeling experiment, $^{13}CO_2$ was applied instead of CO_2 and the product was detected by gas chromatography-mass spectrometry (GC-MS).

Computational Calculations Details:

The energy and structure optimization were performed using DFT calculations, as implemented in the CP2K code of QUICKSTEP module by employing a mixed Gaussian and plane-wave basis sets.[1-3] The electron interactions were described using the generalized gradient approximation (GGA) for the exchange-correlation functional of Perdew, Burke, and Ernzerhof (PBE).[4] The core electrons of transition metal atoms were treated with norm-conserving Goedecker–Teter–Hutter pseudopotentials, and the valence electron wavefunctions were expanded in a double zeta basis sets with polarization functions along with the auxiliary plane wave basis sets.[5-7] The energy cutoff of 450 Ry was used in all calculations. Each reaction intermediate structure was optimized with the Broyden–Fletcher–Goldfarb–Shanno (BGFS) algorithm with the SCF convergence criteria of 1.0×10^{-5} a.u. The DFT-D3 scheme with an empirical damped potential term was added to the electronic energy to account for long-range dispersion interactions.[8]

The adsorption energy between the adsorbate and the substrate can be calculated using the following equation:

$$\Delta E_{ads} = E_{adsorbate@substrate} - E_{substrate} - E_{adsorbate} \qquad (1)$$

In Eq. 1, $E_{adsorbate@substrate}$ and $E_{substrate}$ represent the total energies of the substrate with and without the adsorption of adsorbate respectively. $E_{adsorbate}$ is the total energy of the adsorbate. According to this equation, a negative adsorption energy corresponds to a stable adsorption structure.

In the present work, Gibbs free energy change (G) for each elementary step was calculated using the following equation

$$\Delta G = \Delta E_{elec} + \Delta E_{ZPE} - T\Delta S \qquad (2)$$

where E_{elec} and E_{ZPE} are the electronic term, which is directly derived from DFT calculation, and zero-point energy (*ZPE*) contribution, respectively. *S* is the entropy and *T* is the temperature (298.15 K). E_{ZPE} and *TS* were calculated using the following equations for each reaction intermediates[9],

$$E_{ZPE} = \frac{1}{2}\sum_i h\nu_i \qquad (3)$$

$$-TS = k_B T\sum_i \ln\left(1 - e^{-\frac{h\nu_i}{k_B T}}\right) - \sum_i h\nu_i\left(\frac{1}{e^{\frac{h\nu_i}{k_B T}} - 1}\right) \qquad (4)$$

where k_B is the Boltzmann constant, *h* is Planck's constant and ν_i is vibrational frequencies. The localized harmonic oscillator approximation with a displacement of 0.01 Å was used in the vibrational frequency calculations. During vibrational frequency calculation, only the reaction intermediates were relaxed while all other atoms of the framework were fixed.

2. Figures and Tables

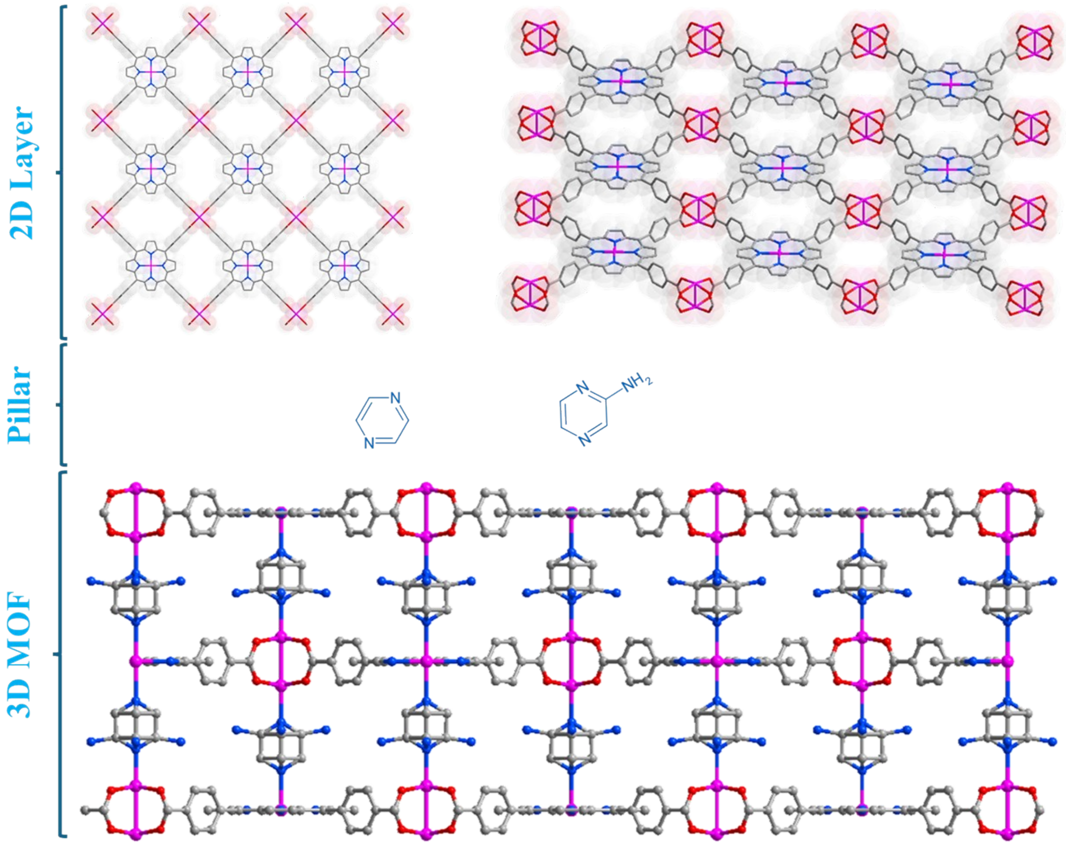

Fig. S1. The self-assembly path of TCPP-Pyz-Co and TCPP-NH_2Pyz-Co.

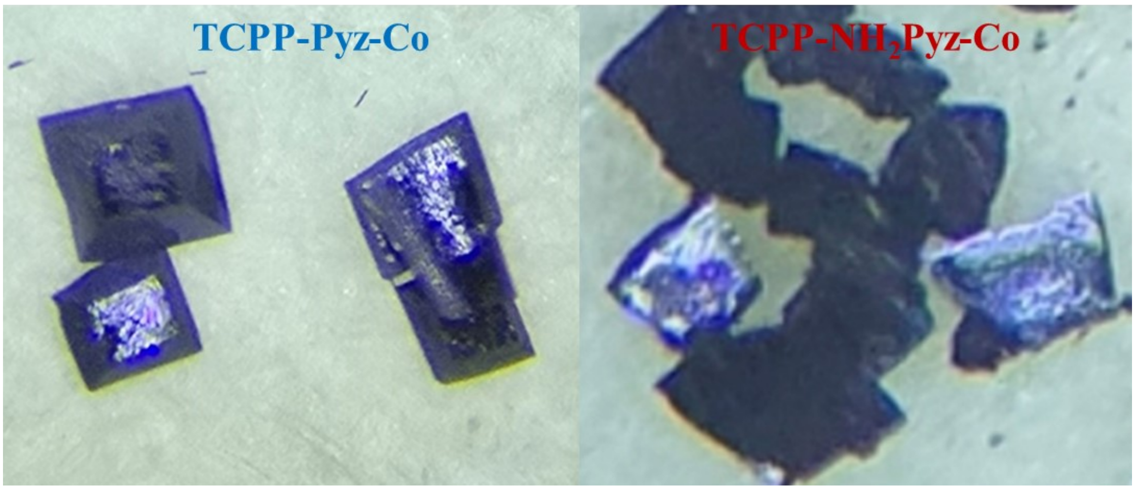

Fig. S2. Optical micrographs of TCPP-Pyz-Co and TCPP-NH_2Pyz-Co single crystals.

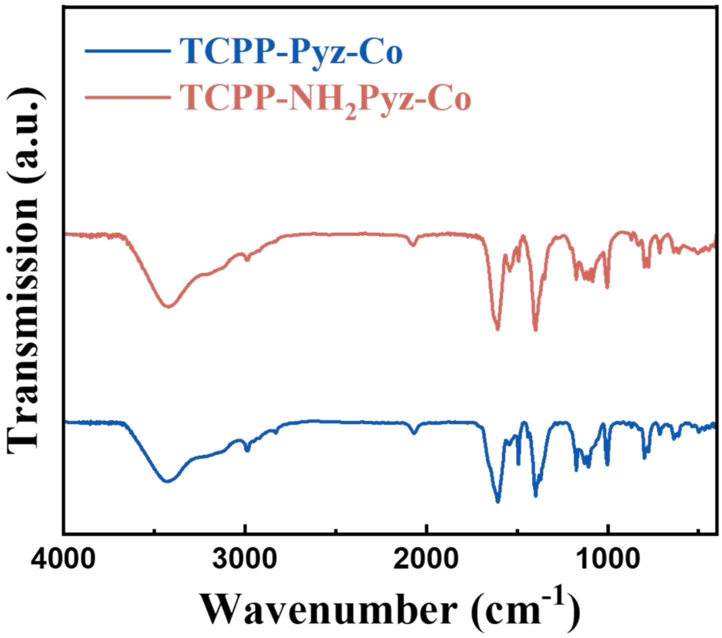

Fig. S3. IR spectra of TCPP-Pyz-Co and TCPP-NH_2Pyz-Co.

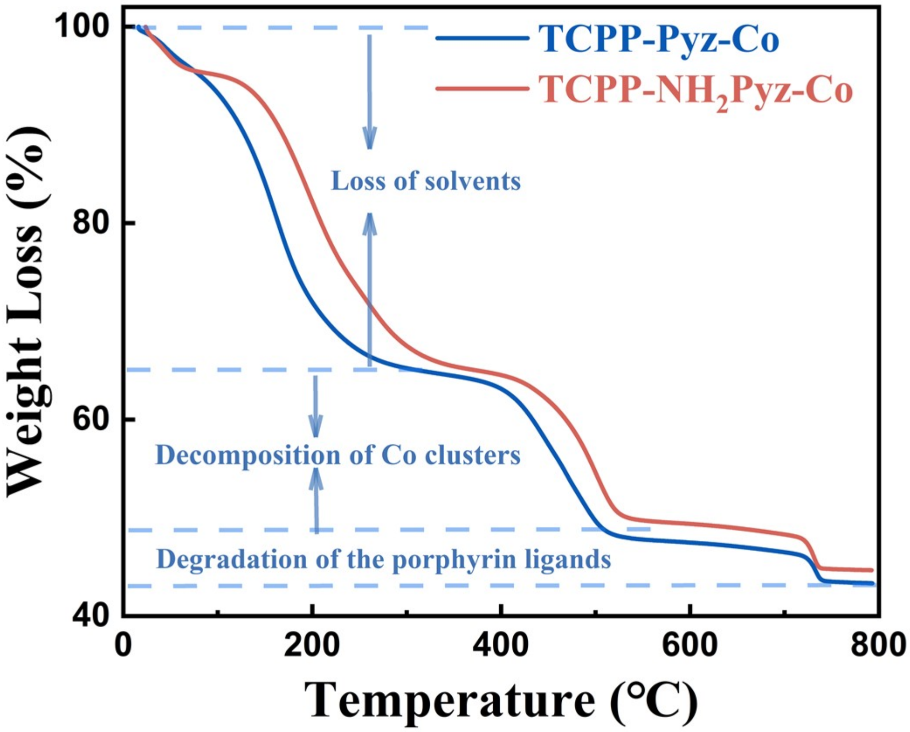

Fig. S4. TGA of TCPP-Pyz-Co and TCPP-NH_2Pyz-Co.

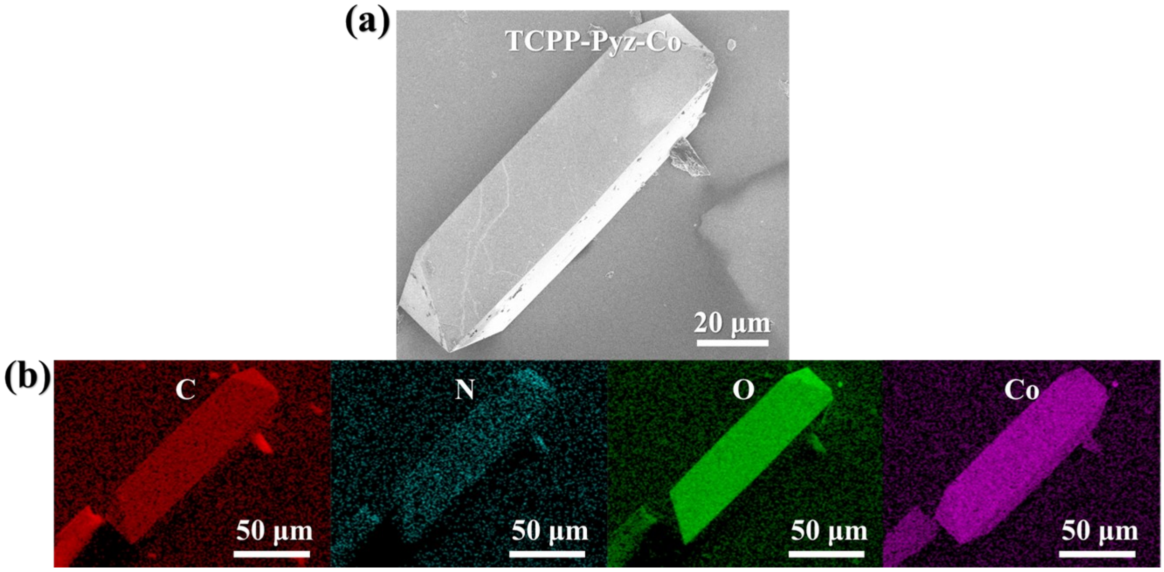

Fig. S5. (a) SEM image and (b) the EDS mapping images of C, N, O, Co elements for TCPP-Pyz-Co.

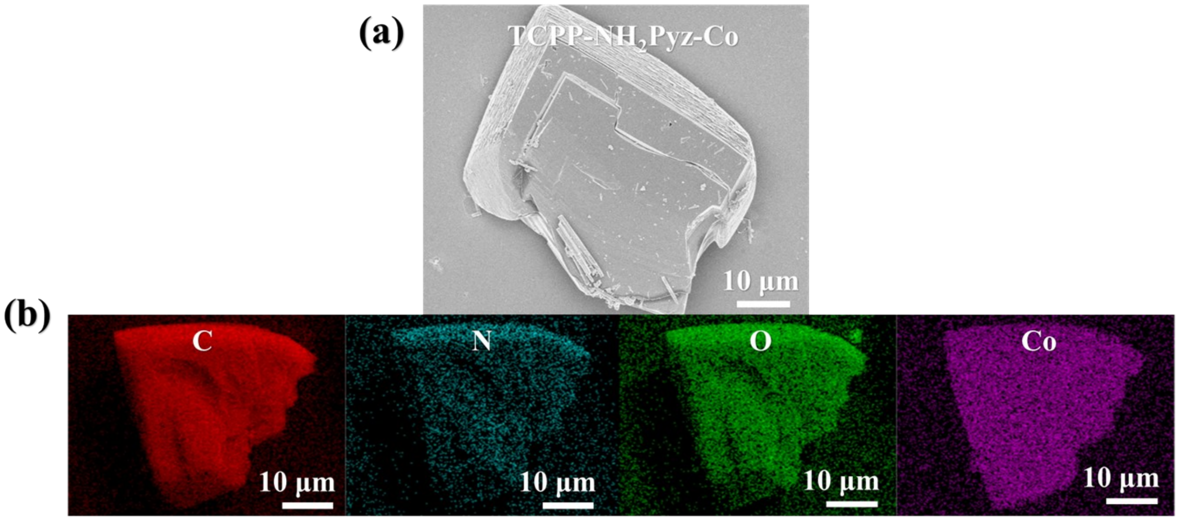

Fig. S6. (a) SEM image and (b) the EDS mapping images of C, N, O, Co elements for TCPP-NH$_2$Pyz-Co.

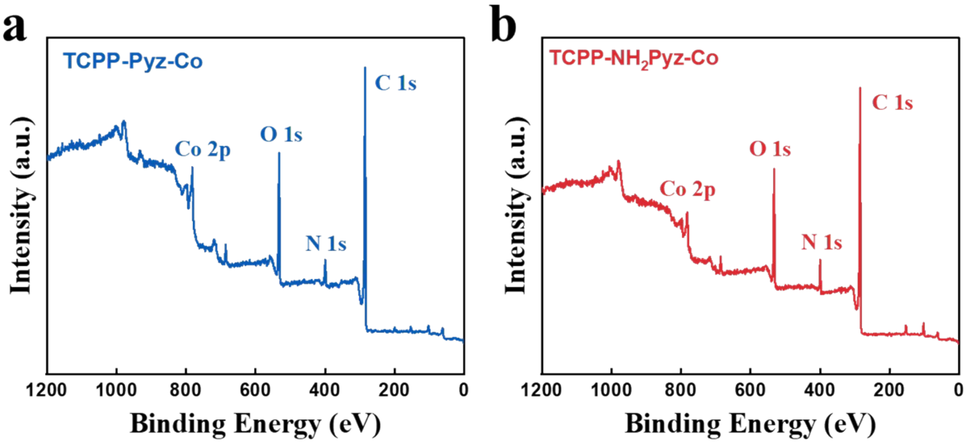

Fig. S7. Survey spectra of (a) TCPP-Pyz-Co and (b) TCPP-NH$_2$Pyz-Co.

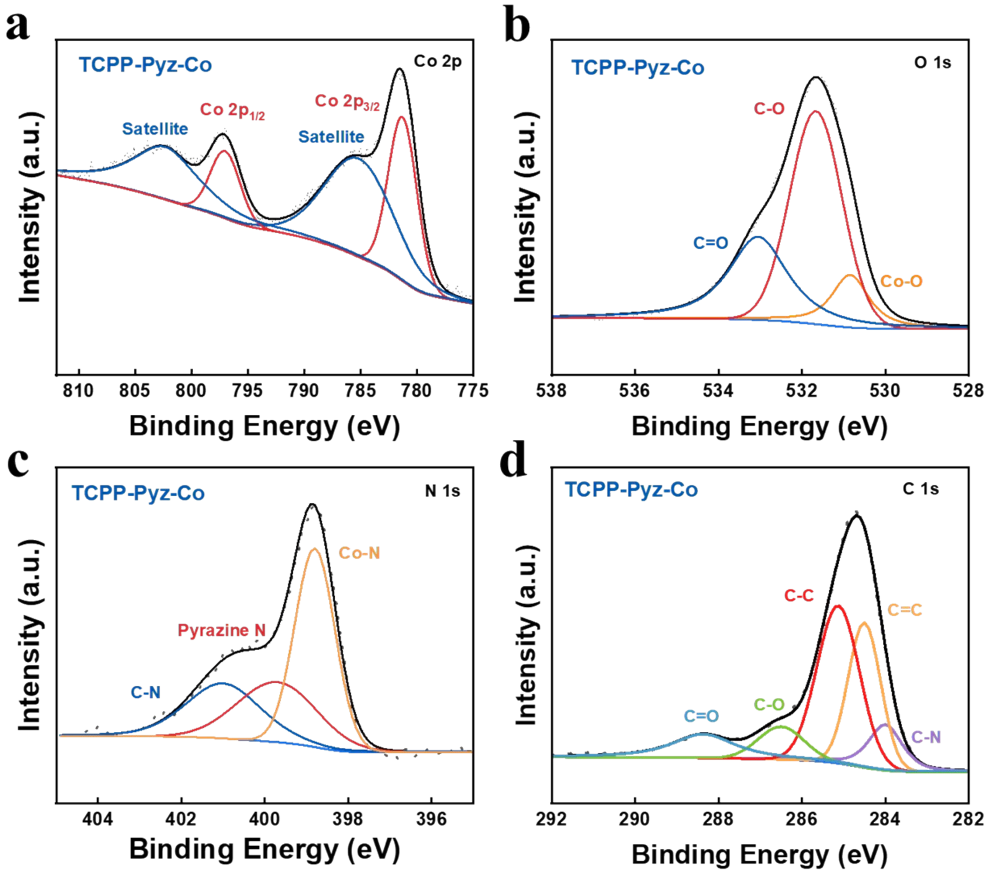

Fig. S8. XPS spectrum of TCPP-Pyz-Co. (a) Co 2p spectrum of TCPP-Pyz-Co, (b) O 1s spectrum of TCPP-Pyz-Co, (c) N 1s spectrum of TCPP-Pyz-Co, (d) C 1s spectrum of TCPP-Pyz-Co.

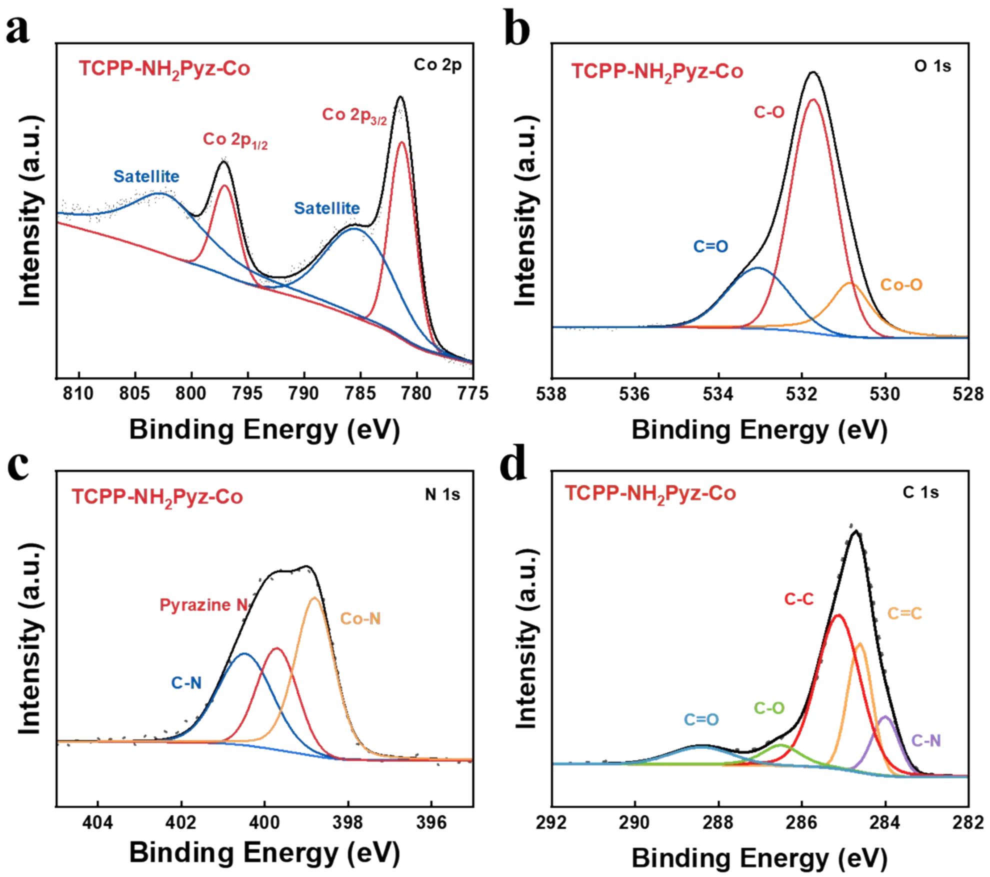

Fig. S9. XPS spectrum of TCPP-NH_2Pyz-Co. (a) Co 2p spectrum of TCPP-NH_2Pyz-Co, (b) O 1s spectrum of TCPP-NH_2Pyz-Co, (c) N 1s spectrum of TCPP-NH_2Pyz-Co, (d) C 1s spectrum of TCPP-NH_2Pyz-Co.

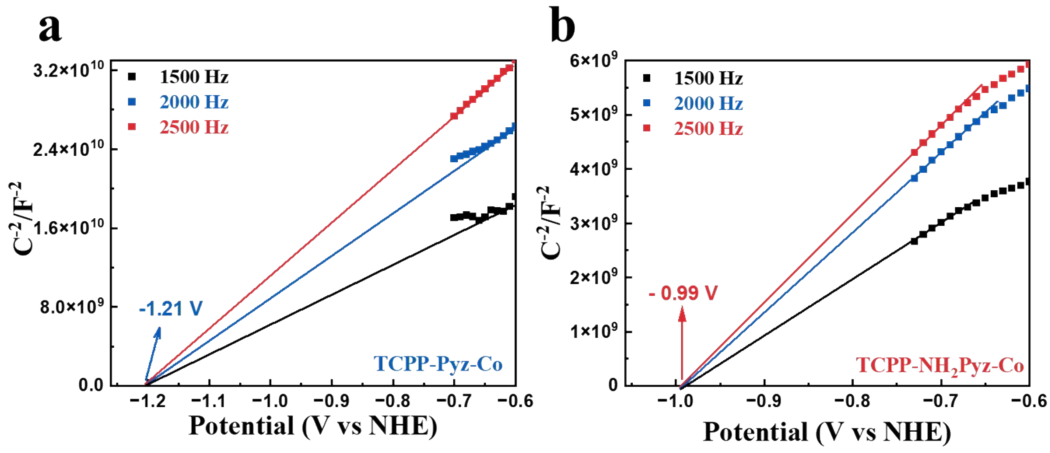

Fig. S10. Mott-Schottky plots of (a) TCPP-Pyz-Co and (b)TCPP-NH_2Pyz-Co.

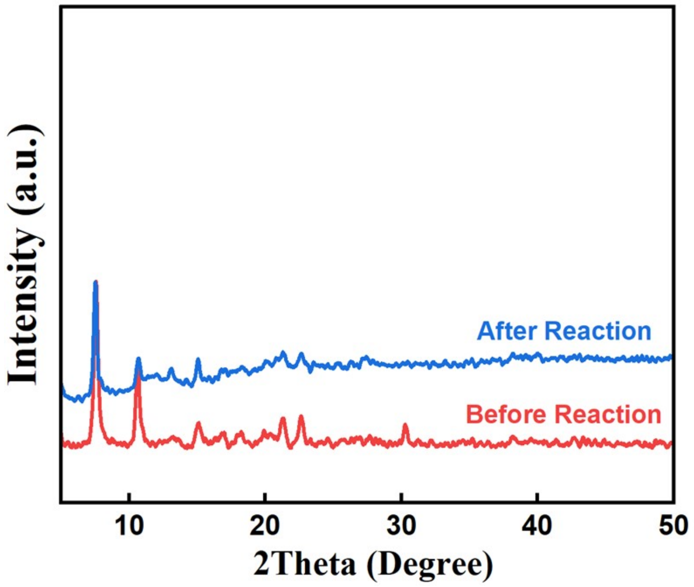

Fig. S11. PXRD pattern of TCPP-NH_2Pyz-Co samples before and after CO_2 reduction reaction.

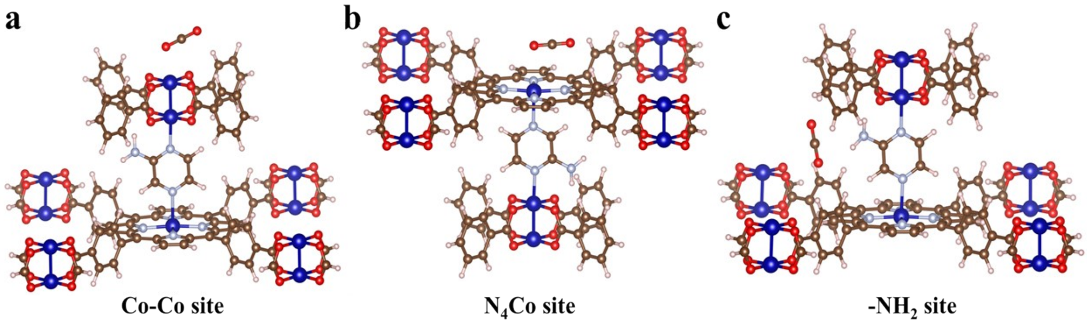

Fig. S12. The DFT-calculated adsorption configuration of CO_2 on TCPP-NH_2Pyz-Co at (a) Co-Co site, (b) N_4Co site and (c) -NH_2 site.

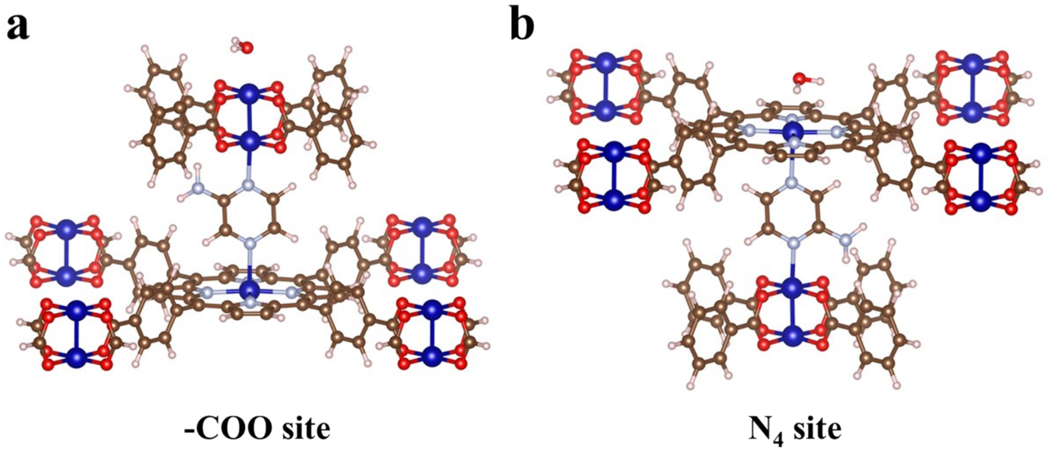

Fig. S13. The DFT-calculated adsorption configuration of H_2O on TCPP-NH_2Pyz-Co at (a) -COO site and (b) N_4 site.

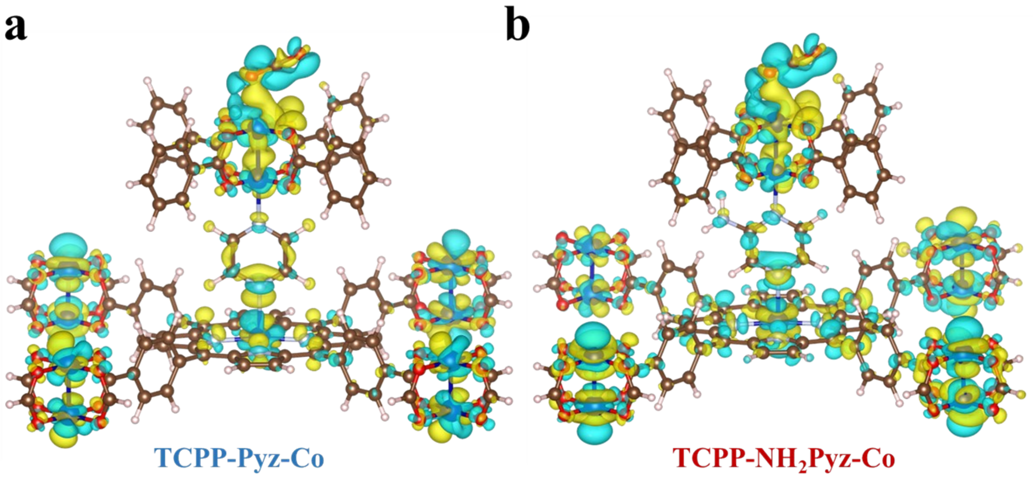

Fig. S14. Charge density difference of CO_2 adsorption on (a) TCPP-Pyz-Co and (b) TCPP-NH$_2$Pyz-Co. Yellow indicates electron accumulation, and light blue indicates depletion.

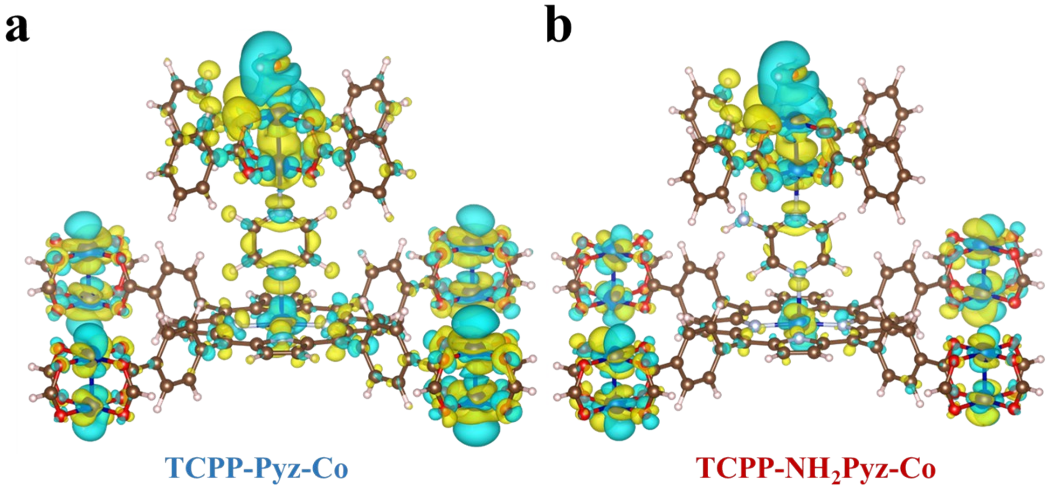

Fig. S15. Charge density difference of H_2O adsorption on (a) TCPP-Pyz-Co and (b) TCPP-NH$_2$Pyz-Co. Yellow indicates electron accumulation, and light blue indicates depletion.

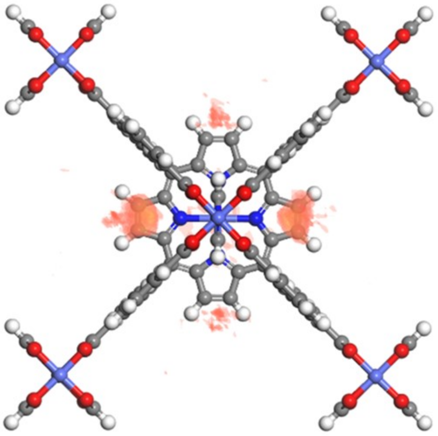

Fig. S16. The CO_2 adsorption density of TCPP-Pyz-Co.

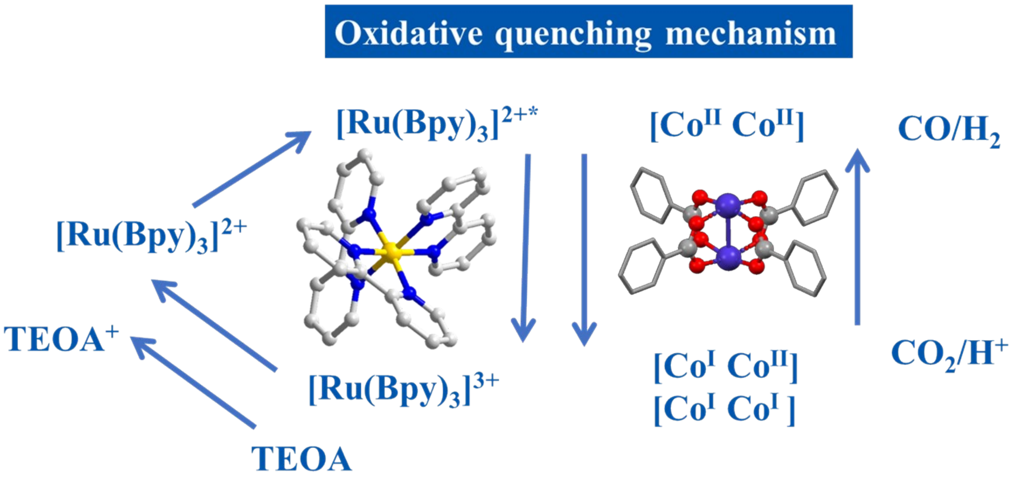

Fig. S17. The oxidative quenching mechanism for $[Ru(bpy)_3]^{2+}$ in the CO_2RR process.

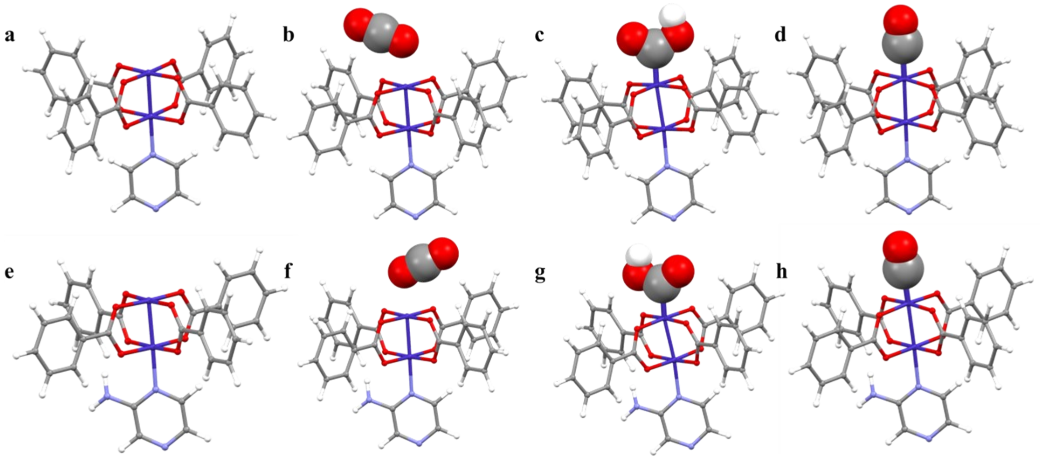

Fig. S18. The detailed configurations of different reaction steps in the CO_2 reduction pathway (a-d) TCPP-Pyz-Co and (e-h) TCPP-NH_2Pyz-Co.

Table S1. Crystal data and structure refinement of TCPP-Pyz-Co and TCPP-NH_2Pyz-Co.

Empirical formula	$C_{112}H_{64}Co_6N_{16}O_{16}$	$C_{56}H_{34}Co_3N_{10}O_8$
Formula weight	2243.37	1151.72
Temperature/K	295.00	279.00
Crystal system	tetragonal	tetragonal
Space group	I4/mmm	I4/mmm
a/Å	16.6853(10)	16.675(7)
b/Å	16.6853(10)	16.675(7)
c/Å	16.7371(11)	17.033(9)
α/°	90	90
β/°	90	90
γ/°	90	90
Volume/Å^3	4659.6(6)	4736(4)
Z	1	2
ρ_{calcg}/cm^3	0.799	0.808
μ/mm^{-1}	0.563	0.555
F(000)	1138.0	1170.0
Radiation	MoKα (λ = 0.71073)	MoKα (λ = 0.71073)
2Θ range for data collection/°	4.868 to 51.892	4.782 to 51.922
Index ranges	$-20 \le h \le 20$, $-20 \le k \le 20$, $-20 \le l \le 20$	$-20 \le h \le 18$, $-20 \le k \le 18$, $-20 \le l \le 20$
Reflections collected	15415	18487
Independent reflections	1327 [R_{int} = 0.0751, R_{sigma} = 0.0274]	1349 [R_{int} = 0.0856, R_{sigma} = 0.0379]
Data/restraints/parameters	1327/18/74	1349/6/80
Goodness-of-fit on F_2	1.052	1.084
Final R indexes [I>=2σ (I)]	R_1 = 0.0525, wR_2 = 0.1409	R_1 = 0.0479, wR_2 = 0.1298
Final R indexes [all data]	R_1 = 0.0627, wR_2 = 0.1509	R_1 = 0.0632, wR_2 = 0.1494
CCDC No.	2447985	2447987

Table S2. The peak area ratio changes calculated from the N 1s spectrum of TCPP-Pyz-Co and TCPP-NH_2Pyz-Co.

N species	TCPP-Pyz-Co Integral area	TCPP-Pyz-Co Percentage	TCPP-NH_2Pyz-Co Integral area	TCPP-NH_2Pyz-Co Percentage
C-N	2881.19	26.5%	3730.91	31.84%
Pyrazine N	3003.23	27.6%	2957.49	25.24%
Co-N	4990.35	45.9%	5027.73	42.92%

Table S3. Summary of TCPP-NH_2Pyz-Co adsorbents and the corresponding CO_2 capture capacity.

Adsorbent	Pressure (bar)	Temperature (K)	Capacity (mmol/g)	Reference
MOF-808-Gly	1	298	2.03	10
Zr-tcpb-COOCa	1	298	1.48	11
Zr-UiO-66	1	273	2.88	12
Zr-IAM-4	1	298	1.58	13
MOF-553	1.1	273	3.7	14
NH_2-Zr(H_2L)	1	273	2.45	15
NU-1008	1	298	0.08	16
MOF-808@N	10	298	5.6	17
VPI-100 (Cu)	1	273	1.51	18
CO_2–Zr-DEP	1	273	2.91	19
Hf-VPI-100 (Cu)	1	273	1.87	20
JLU-Liu45	1	273	5.17	21
UiO-67-ILs-Cl	1	273	3.8	22
TCPP-NH_2Pyz-Co	**1**	**298**	**2.18**	**This work**

Table S4. Control experiments of CO_2 reduction reaction for TCPP-NH_2Pyz-Co catalyst.

	CO (μmol g^{-1} h^{-1})	H_2 (μmol g^{-1} h^{-1})
Without Light	0	0
Without Catalyst	0	0
Without Ru(bpy)$_3^{2+}$	200	50
Without TEOA	0	0

Table S5. Comparison of photocatalytic CO_2 reduction to CO property with recently reported porphyrin-based MOFs.

Photocatalyst	Light source	Solvent	Photosensitizer	Sacrificial Agent	Major Products	CO generation rate (μmol/g/h)	Ref.
PCN-222	300 W Xe lamp	-	-	-	CO, CH_4	5.5	23
PCN-601						6.0	
MOF-525-Co	300 W Xe lamp	MeCN, H_2O	-	TEOA	CO, CH_4	200.6	24
MOF-525-Zn						111.7	
MOF-525						64.2	
ZrPP-1-Co	300 W Xe lamp	MeCN	-	TEOA	CO, CH_4	14	25
BUT-110-50%-Fe	300 W Xe lamp	H_2O	-	TEA	CO, CH_4	47.2	26
BUT-110-50%-Ni	300 W Xe lamp	H_2O	-	TEA	CO, CH_4	24.6	
BUT-110-50%-Co	300 W Xe lamp	H_2O	-	TEA	CO, CH_4	64	
BUT-110-50%-Cu	300 W Xe lamp	H_2O	-	TEA	CO, CH_4	55.8	
bilayer MOF	300 W Xe lamp	MeCN, H_2O	-	TEOA	CO	276.8	27
Zn-based PMOF	300 W Xe lamp	H_2O	-	-	CO, CH_4	14	28
Co-MOF-1	300 W Xe lamp	H_2O	$[Ru(bpy)_3]Cl_2$	TEOA	CO	10.7	29
Co-MOF-3						27.1	
IHEP-21	300 W	MeCN	-	TEOA	CO, CH_4	38.6	30
IHEP-22	Xe lamp	MeCN	-	TEOA	CO, CH_4	143.8	
IHEP-23	300 W	MeCN	-	TEOA	CO, CH_4	119.2	
IHEP-21(Co)	Xe lamp	MeCN	-	TEOA	CO, CH_4	97.5	
IHEP-22(Co)	300 W	MeCN	-	TEOA	CO, CH_4	350.9	
IHEP-23(Co)	Xe lamp	MeCN	-	TEOA	CO, CH_4	240.3	
TCPP-Pyz-Co	300 W Xe lamp	MeCN, H_2O	$[Ru(bpy)_3]Cl_2$	TEOA	CO, H_2	1807.6	This work
TCPP-NH_2Pyz-Co	300 W Xe lamp	MeCN, H_2O	$[Ru(bpy)_3]Cl_2$	TEOA	CO, H_2	2221.4	

3. References

(1) M. Krack and M. Parrinello, *Phys. Chem. Chem. Phys.*, 2000, **2**, 2105-2112.

(2) T. D. Kühne, M. Iannuzzi, M. Del Ben, V. V. Rybkin, P. Seewald, F. Stein, T. Laino, R. Z. Khaliullin, O. Schütt, F. Schiffmann, D. Golze, J. Wilhelm, S. Chulkov, M. H. Bani-Hashemian, V. Weber, U. Borštnik, M. Taillefumier, A. S. Jakobovits, A. Lazzaro and H. Pabst, *J. Chem. Phys.*, 2020, **152**, 194103.

(3) J. VandeVondele, M. Krack, F. Mohamed, M. Parrinello, T. Chassaing and J. Hutter, *Comput. Phys. Commun.*, 2005, **167**, 103–128.

(4) J. P. Perdew, K. Burke and M. Ernzerhof, *Phys. Rev. Lett.*, 1996, **77**, 3865–3868.

(5) J. VandeVondele and J. Hutter, *J. Chem. Phys.*, 2007, **127**, 114105.

(6) S. Goedecker, M. Teter and J. Hutter, *Phys. Rev. B*, 1996, **54**, 1703–1710.

(7) C. Hartwigsen, S. Goedecker and J. Hutter, *Phys. Rev. B*, 1998, **58**, 3641–3662.

(8) S. Grimme, J. Antony, S. Ehrlich and H. Krieg, *J. Chem. Phys.*, 2010, **132**, 154104.

(9) C. Ling, X. Niu, Q. Li, A. Du and J. Wang, *J. Am. Chem. Soc.*, 2018, **140**, 14161–14168.

(10) H. Lyu, O. I.-F. Chen, N. Hanikel, M. I. Hossain, R. W. Flaig, X. Pei, A. Amin, M. D. Doherty, R. K. Impastato, T. G. Glover, D. R. Moore and O. M. Yaghi, *J. Am. Chem. Soc.*, 2022, **144**, 2387-2396.

(11) G. Zhang, F. Xie, T. M. Osborn, A. Patel, Eder, K. Tan, R. Crichton, G. Hall, J. Zhang, A. J. Nieuwkoop and J. Li, *CrystEngComm*, 2023, **25**, 1067-1075.

(12) J. Du, L. Chen, X. Zeng, S. Yu, W. Zhou, L. Tan, L. Dong, C. Zhou and J. Cheng, *ACS Appl. Mater. Inter.*, 2020, **12**, 28576-28585.

(13) Z. Duan, Y. Li, X. Xiao, X. Huang, X. Li, Y. Li, C. Zhang, H. Zhang, L. Li, Z. Lin, Y. Zhao and W. Huang, *ACS Appl. Mater. Inter.*, 2020, **12**, 18715-18722.

(14) S. Demir, N. Bilgin, H. M. Cepni, H. Furukawa, F. Yilmaz, C. Altintas and S. Keskin, *Dalton Trans.*, 2021, **50**, 16587-16592.

(15) X. Sun, L. Shi, H. Hu, H. Huang and T. Ma, *Adv. Sustain. Syst.*, 2020, **4**, 2000098.

(16) J. Lyu, X. Zhang, K. Otake, X. Wang, P. Li, Z. Li, Z. Chen, Y. Zhang, M. C. Wasson, Y. Yang, P. Bai, X. Guo, Timur Islamoglu and O. K. Farha, *Chem. Sci.*, 2018, **10**, 1186-1192.

(17) H. N. Wamba, Suman Dalakoti, N. Singh, Swapnil Divekar, J. Ngoune, A. Arya and S. Dasgupta, *Ind. Eng. Chem. Res.*, 2023, **62**, 19773-19783.

(18) J. Zhu, P. M. Usov, W. Xu, P. J. Celis-Salazar, S. Lin, M. C. Kessinger, C. Landaverde-Alvarado, M. Cai, A. M. May, C. Slebodnick, De Hua Zhu, S. D. Senanayake and Amanda Sheffield Morris, *J. Am. Chem. Soc.*, 2018, **140**, 993-1003.

(19) B. Song, Y. Liang, Y. Zhou, L. Zhang, H. Li, N.-X. Zhu, Ben Zhong Tang, D. Zhao and B. Liu, *J. Am. Chem. Soc.*, 2024, **146**, 14835-14843.

(20) J. Zhu, J. Liu, Y. Machain, B. Bonnett, S. Lin, M. Cai, M. C. Kessinger, P. M. Usov, W. Xu, S. D. Senanayake, D. Troya, A. R. Esker and A. J. Morris, *J. Mater. Chem. A*, 2018, **6**, 22195-22203.

(21) X. Sun, X. Li, S. Yao, R. Krishna, J. Gu, G. Li and Y. Liu, *J. Mater. Chem. A*, 2020, **8**, 17106-17112.

(22) W.-L. Xue, L. Wang, Y. K. Li, H. Chen, K. X. Fu, F. Zhang, T. He, Y. H. Deng, J. R. Li and C.-Q. Wan, *ACS Sustain. Chem. Eng.*, 2020, **8**, 18558-18567.

(23) Z.-B. Fang, T.-T. Liu, J. Liu, S. Jin, X.-P. Wu, X.-Q. Gong, K. Wang, Q. Yin, T.-F. Liu, R. Cao and H.-C. Zhou, *J. Am. Chem. Soc.*, 2020, **142**, 12515–12523.

(24) H. Zhang, J. Wei, J. Dong, G. Liu, L. Shi, P. An, G. Zhao, J. Kong, X. Wang, X. Meng, J. Zhang and J. Ye, *Angew. Chem. Int. Ed.*, 2016, **55**, 14310–14314.

(25) E.-X. Chen, M. Qiu, Y.-F. Zhang, Y.-S. Zhu, L.-Y. Liu, Y.-Y. Sun, X. Bu, J. Zhang and Q. Lin, *Adv. Mater.*, 2017, **30**, 1704388.

(26) X. Kong, T. He, J. Zhou, C. Zhao, T. Li, X. Wu, K. Wang and J. Li, *Small*, 2021, **17**, 2005357.

(27) J. Liang, H. Yu, J. Shi, B. Li, L. Wu and M. Wang, *Adv. Mater.*, 2023, **35**, 2209814–2209814.

(28) J.-H. Qin, Z. Xiao, P. Xu, Z.-H. Li, X. Lu, X.-G. Yang, W. Lu, L.-F. Ma and D.-S. Li, *Inorg. Chem.*, 2022, **61**, 13234–13238.

(29) Y. Liu, C. Chen, J. Valdez, Débora Motta Meira, W. He, Y. Wang, Cătălin Harnagea, Q. Lu, Tuğrul Güner, H. Wang, C. Liu, Q. Zhang, S. Huang, Aycan Yurtsever, M. Chaker and D. Ma, *Nat. Commun.*, 2021, **12**, 1231.

(30) Z. Huang, K. Hu, X. Li, Z.-N. Bin, Q. Wu, Z. Zhang, Z. Guo, W. Wu, Z. Chai, L. Mei and W. Shi, *J. Am. Chem. Soc.*, 2023, **145**, 18148–18159.